International Journal of Industrial Chemistry (IJIC)
a SpringerOpen Journal

REVIEW Open Access

Micelles, mixed micelles, and applications of polyoxypropylene (PPO)-polyoxyethylene (PEO)-polyoxypropylene (PPO) triblock polymers

Vijender Singh[1,2], Poonam Khullar[2], Pragnesh N Dave[1*] and Navjot Kaur[3]

Abstract

This review gives a brief outline of various micellar properties of triblock polymers such as critical micellization concentration, critical micellization temperature, and microviscosity. Detailed discussion of the effect of temperature on micellar properties of various triblock polymer mixtures is given. Applications of triblock polymers in solubilization as drug delivery agents, as nano drug, for the synthesis of gold nanoparticles, for cobalt determination, etc. are discussed.

Keywords: Micellization, Critical micelle concentration, Cloud point, Critical micelle temperature

Review

Characteristic features of triblock polymers

Triblock polymers (TBPs) also known as block copolymers belong to a class of nonionic surfactants. They are commercially available under the trade names Pluronics (BASF, Ludwigshafen, Germany), Poloxamers (ICI, London, England), or Synperonics (ICI) and are highly surface-active compounds. The block copolymers consist of a linear hydrophobic polyoxypropylene (PPO) block with hydrophilic polyoxyethylene (PEO) blocks on each side with the structure PEO-PPO-PEO. Their hydrophilic-lipophilic balance (HLB) depends on the PEO-to-PPO mass ratio [1,2]. The rich polymorphic behavior of Pluronics is modulated by their HLB [3]. The PEO-PPO-PEO TBPs are commercially available in a range of molecular weights and PPO-PEO composition [4]. Greater amount of oxyethylene groups, for instance, implies significant aqueous solubility. TBPs are the subjects of fundamental as well as technological research [5-7] that arises from their ability to form micelles, macro- or micro emulsions, and several liquid crystalline phases [8-10]. Because of low toxicity and high biodegradability, these copolymers have extensive industrial applications in detergency, paint industries [11], cosmetics, dispersion stabilization, foaming, lubrication [12,13], and pharmaceutical formulation [14,15]. Other important applications include radiation-damaged cell repair and treatments, controlled drug delivery, bioprocessing [16], nuclear waste processing [17,18], food processing, as well as in agricultural formulations [19-21]. Further applications are emulsion [22] and stabilization in polymerization reaction [23], nanomaterial synthesis [24,25], and coal processing [26].

Fundamentally, they have tremendous advantages than conventional neutral polymers due to the presence of both hydrophilic (i.e., PEO) and hydrophobic predominant (i.e., PPO) moieties in the same polymer molecule. In analogy with the low molecular weight surfactants [27], block copolymers form aggregates of different kinds, depending on the molecular weight, block sizes, solvent composition, and temperature. The low molecular weight Pluronics are viscous oils or pastes, and high molecular weight Pluronics are amorphous solids. The different types of blocks within the copolymer are usually incompatible with one another, and as a consequence, block copolymers self-assemble in melts and in solutions. They also show anomalous behavior over a certain range of temperature, an effect shown, in general, by block copolymers in selective solvents [28,29] which has been found due to the presence of more hydrophobic component present as impurity [30,31].

* Correspondence: pragnesh7@yahoo.com
[1]Department of Chemistry, KSKV Kachchh University, Bhuj, Gujarat 370001, India
Full list of author information is available at the end of the article

Micellization

Critical micelle concentration

The parameter of greatest fundamental value is the critical micellization concentration (CMC), the copolymer concentration at which micelles start forming [32]. TBPs are the nonionic surfactants, which limit the number of techniques available to measure the CMC in comparison to those of ionic surfactants. Also in comparison with conventional low molecular weight surfactants, there is some inherent complexity in the micellization of block copolymers, which depends strongly on their composition [33-42]. The blocks are not completely monodisperse even for a copolymer with a narrow distribution of molecular weight, and accordingly, no sharp CMC/critical micellization temperature (CMT) has been observed for block copolymers. Generally, the CMC spans over a much larger concentration interval than observed with conventional surfactants. The CMC is also sensitive to the temperature which is likely to extend the concentration range over which the CMC occurs [33]. Various techniques such as light scattering [33,43], fluorescence spectroscopy [44,45], NMR [46], specific volume [47,48], and small-angle neutron scattering (SANS) [49,50] have been frequently used to gain new insight into the aggregation behavior of these systems. The process of self-association can be induced by increasing the concentration of TBPs above the CMC and adjusting the temperature to CMT [30,51-56].

Micellization in TBPs is understood to arise due to the following reasons [29,57]. As the temperature of a block copolymer solution is raised, the PPO block progressively loses its hydration sphere, resulting in greater interactions between the PPO blocks. On the other hand, the PEO blocks retain their strong interaction with water; thus as is common for all amphiphilic molecules, the differing phase preferences of the blocks drive the copolymers to form micelles. Structural studies [31,58-63] have shown that the micelles form a hydrophobic core consisting mainly of weakly hydrated PPO blocks, which are surrounded by an outer shell known as corona of almost fully hydrated PEO blocks (Figure 1). There is a broad temperature range above the CMT where the micelles coexist in a solution with unimers. Above the transition region, most of the block copolymer molecules form micelles [64-71]. The reason that a higher temperature is needed to form micelles is that the effective PEO-PEO, PPO-PPO, and PEO-PPO interactions are temperature-dependent. At some temperature, the effective PPO-PPO attraction will dominate over the PEO-PEO repulsion, and micelles will form (Figure 1). CMT of some common triblock polymer is listed in Table 1.

Micelle formation is an extremely temperature-dependent entropy-driven process resulting in a large decrease in CMC upon increasing the temperature. This behavior has led to the wide applicability of CMT as a convenient

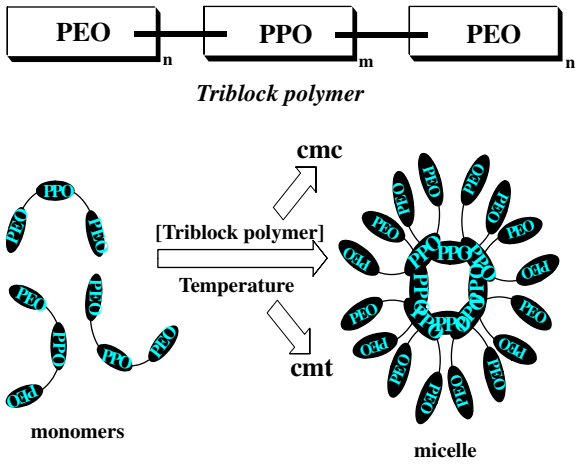

Figure 1 Schematic representation of the general structure of triblock polymer and micelle formation. With respect to the increase in the concentration and temperature.

micellar parameter. Above the CMT, unimers and micelles exist in the state of equilibrium with most of the copolymer molecules in the micellar form. The effects of temperatures on the properties and structure of the PEO-PPO-PEO copolymer solution have been studied extensively [59,72]. An interesting property of the aqueous micellar system is its ability to enhance the solubility in water of otherwise water-insoluble hydrophobic compounds. This occurs because the core of the micelle provides a hydrophobic microenvironment suitable for solubilizing such molecules.

Many of these copolymers associate in aqueous solution to form spherical micelles [8,59,73], while at higher concentration, block copolymers can also self-assemble into lyotropic liquid crystals [54,74,75]. The progressive growth of the hydrophobic core with increasing temperature due to the increasing dehydration of PEO blocks in the corona induces instability in the spherical micellar dispersion, leading to the formation of rod-like structures. The addition of multivalent salts to aqueous copolymer solutions produces a dramatic effect on the transformation of

Table 1 CMT data 0.1% solution of TBPs

TBPs	Concentration (mM)	CMT (°C)
L64	0.345	39.5
P65	0.294	46
P84	0.238	37
P85	0.217	37.5
F88	0.088	48.5
P103	0.202	24.5
P104	0.169	27.5
P105	0.154	27
F108	0.068	36

the copolymer [76]. At low concentration, spherical micelles form, whereas at high concentration, the formation of hexagonal, cubic, and lamellar liquid crystalline phases takes place [58]. The morphology spectrum runs from micelles (L1), through a cubic array of micelles (I1), hexagonally packed rods (H1), and cubic bicontinuous spheres (V1), to lamellae (L3) where phase inversion takes place, and the inverted morphologies develop: cubic (V2), reversed hexagonal (H2), cubic (I2), and reversed micelle (L2) [77,78]. Regular micelles are formed in polar solvents such as water and alcohols; thus, the corona has a hydrophilic character. Micelles formed in nonpolar solvents such as toluene have a hydrophobic corona and are referred to as 'reverse.' Recently, much attention has been devoted to highly asymmetric block copolymers that form aggregates characterized by a large core and a thin coronal shell of the soluble block: the crew-cut systems [79,80]. 'Crew-cut' micelle-like aggregates represent a new type of aggregate. They are formed via the self-assembly of a highly asymmetric amphiphilic block copolymer, in which the insoluble core-forming blocks are much longer than the soluble corona-forming blocks [81,82]. One of the noteworthy phenomena associated with crew-cut aggregates is the accessibility of a wide range of morphologies [79,81,83,84]. These include spheres, rods, vesicles, lamellae, large compound micelles, large compound vesicles, a hexagonally packed hollow hoop structure (the 'HHH' structure) [85], onions [86], a bowl-shaped structure [87], and several others [88,89].

Cloud point and microviscosity

Another parameter of great practical importance of TBPs in aqueous phase is the cloud point (C_P) [73,90,91]. At higher temperatures well above the CMT, the copolymer solution becomes opaque because the phase separation between the polymer and water occurs. The temperature at which cloudiness appears due to the precipitation is the C_P of TBPs [92,93]. The C_P phenomenon in TBPs is related to the core and corona model of the TBP aggregates. This model suggests that the core of TBP micelles mainly consists of PPO units while the corona occupies PEO units. The presence of ether oxygens both in the PPO as well as PEO units allows some number of water molecules to be even available in the core. An increase in the temperature thus dehydrates the TBP micelles even at optimum temperatures by expelling water molecules, which are weakly associated with ether oxygens through the electrostatic interactions. At C_P, the attractive interactions between PEO blocks and water molecules are sufficiently weak that the PEO blocks become completely dehydrated. It has been observed [94,95] that any factor which would increase the number of water molecules in TBP micelles would result in an increase in C_P and vice versa. The TBPs containing a larger PPO block than that of PEO have higher microviscosity [96-98]. The microviscosity is strongly affected by the PPO block. It appears that the larger its molecular weight, the more viscous the micelle interior. Among the two different polymers, the micelles with a larger PPO block exhibit higher microviscoscity. Cloud point of some common triblock polymer solutions of 1% concentration is cited in Table 2.

Mixed micelles

Like conventional surfactants, TBPs show a clear micelle formation process which can be best demonstrated by the change in I_1/I_3 pyrene ratio versus concentration plots. Since the anterior of the TBP micelle is constituted by the predominantly hydrophobic PPO units surrounded by hydrophilic PEO, therefore pyrene can easily solubilize in the core of the micelle and hence can act as a fine probe for the micelle formation process. The I_1/I_3 ratio is sensitive to the microenvironment of pyrene solubilization, and hence, its variation explains the micelle formation process. In aqueous TBP solutions (Figure 2), it usually starts from approximately 1.75 (value in pure water) and decreases to a constant value around 1.3 where it is solubilized in the TBP micelle. Similar methods can very well be adopted for the measurements of CMC for the mixed components over the whole mole fraction range.

P103 + TBPs mixtures

P103 consists of 60 PO units in comparison to 34 EO units. It makes this TBP predominantly nonpolar. The variation of mixed CMC values for different mixtures of P103 is shown in (Figure 3) along with the ideal mixing. It is usually difficult to determine from the CMC profiles which mixture shows greater attractive or repulsive

Table 2 Cloud point of 1% solution of TBPs

TBPs	Cloud point (°C)
L35	73
F38	>100
L42	37
L43	42
L44	65
L62	32
L63	34
P84	74
P85	85
F127	>100
P123	90
L122	19
L64	58
P103	86

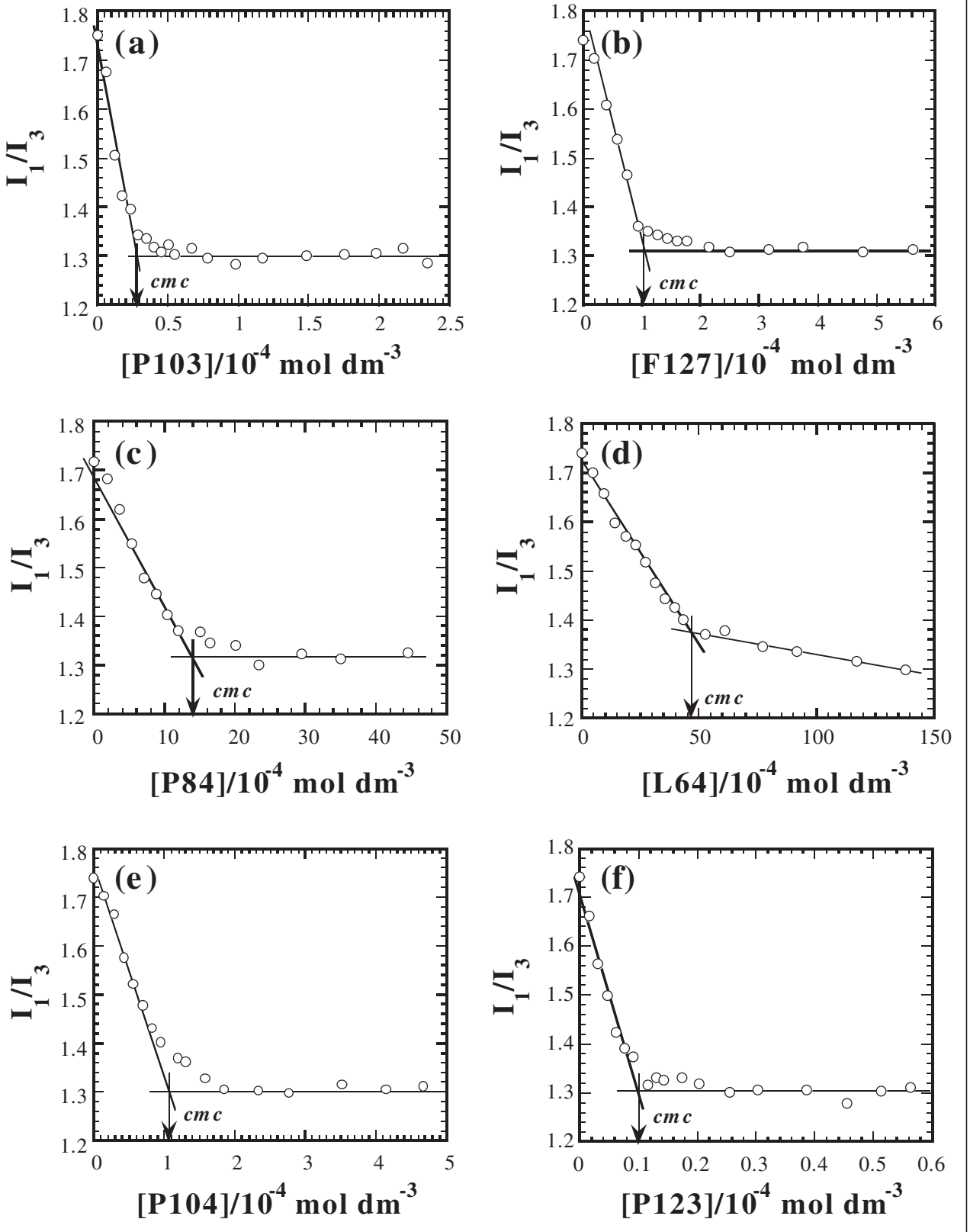

Figure 2 Critical micelle concentration of different TBPs.

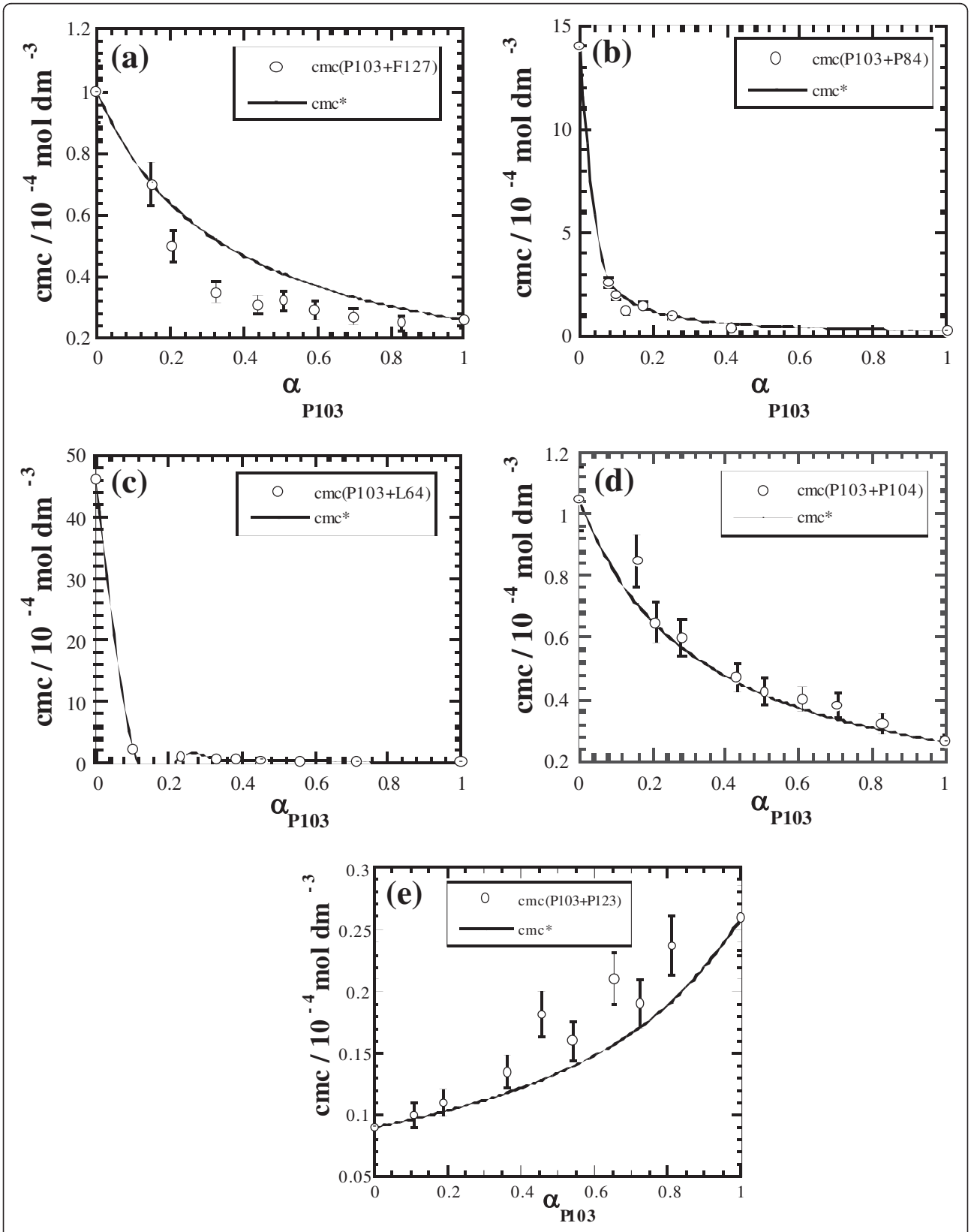

Figure 3 Critical micelle concentration versus mole fraction of P103. For (**a**) P103 + F127, (**b**) P103 + P84, (**c**) P103 + L64, (**d**) P103 + P104, and (**e**) P103 + P123 binary mixtures, respectively.

interactions due to the course of micellization; therefore, the regular solution theory based on the ideal mixing is the best way to establish the non-ideal behavior in terms of parameter 'β.' The average of β values over different mixing ratios for each mixture helps to understand the fact on how one mixture of intermolecular interactions is different from other mixtures. Average β values plotted against the PPO/PEO ratio for different mixtures are shown in (Figure 4). A positive and negative value respectively indicates the operating repulsive and attractive interactions between the components of the mixtures. β_{Avg} becomes more negative as PPO/PEO increases and approaches 1.5. Further increase in the PPO/PEO ratio instantaneously converts β_{Avg} from a negative to a positive value. Components with lower PPO/PEO ratio (i.e., F127, P84, and L64) show attractive interactions with P103, while the component with greater PPO/PEO ratio (i.e., P104 and P123) shows unfavorable mixing with P103 which is clearly related to the delicate balance between the PO and EO units in a mixed state. P103 contains a greater number of PO (70) units in comparison to EO (38) units which makes P103 a predominantly hydrophobic polymer. Thus, in the event of micelle formation with other TBPs, P103 will prefer to have maximum synergistic mixing with similar predominantly hydrophobic TBPs such as L64 rather than P104 and P123 with much higher number of PO units in comparison to EO which will induce steric effects in the core, resulting in the unfavorable mixing.

Temperature effect on P103 + F127/P123 mixtures

Temperature is another very important parameter which can drastically affect the microenvironment of the TBP micelle. PO units show dramatic loss of water or hydration in comparison to EO units as temperature increases. In the first combination, the relative difference between the molecular weights of PPO blocks of P103 and F127 is much less in comparison to that among PEO blocks. In the latter case, this difference is more significant for PPO blocks rather than that of PEO blocks. Hence, we want to see which combination of these two would produce greater non-ideal behavior (favorable or unfavorable) in their mixed state and also under the effect of temperature variation.

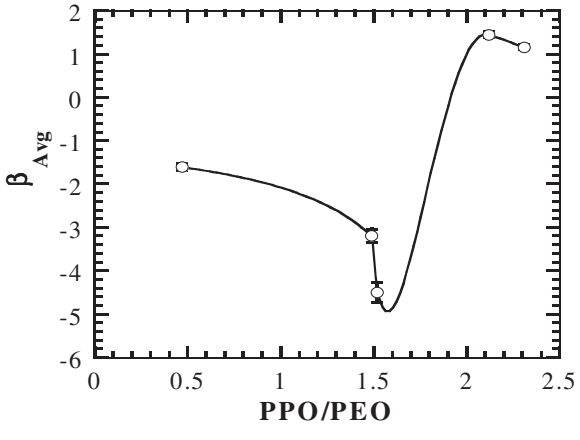

Figure 4 Plot of interaction parameter, β_{Avg}, versus PPO/PEO ratio of the triblock polymers.

The mixed CMC values are shown graphically in Figures 5 and 6 along with the ideal CMC values. The experimental CMC values for the P103 + F127 mixture (Figure 5) are lower than the ideal behavior at 25°C, and this difference decreases as the temperature increases from 25°C to 40°C. In contrast, the experimental values are quite close to the ideal ones for the P103 + P123 mixture (Figure 6) at 25°C but become significantly higher as temperature increases. It means that P103 + F127 shows attractive interactions at 25°C that decrease with the temperature, while P103 + P123, on the other hand, behaves almost ideally at 25°C but becomes increasingly non-ideal as temperatures increases. Since the temperature variation has a dramatic effect on the hydration of mixed TBP micelles, therefore, this effect should reflect from the viscosity measurements. Plots of excess relative viscosity ($\Delta\eta_{\mathrm{r}}$) of both mixtures over the whole mole fraction range (Figure 7) demonstrate negative deviation at 25°C for P103 + F127 that decreases as the temperature increases, while at 40°C, it almost follows the additivity rule. Whereas, $\Delta\eta_{\mathrm{r}}$ for P103 + P123 mixtures shows a comparatively very weak negative deviation at 25°C from an ideal behavior that decreases and reverts to a weak positive deviation as temperature increases.

The negative deviations in $\Delta\eta_{\mathrm{r}}$ values generally arise from the decrease in fluidity in the bulk upon mixing two components. That is happening due to attractive interactions between the micelles of P103 and F127 in order to form mixed micelles which enhance the aggregation, and hence, a greater number of aggregates reduce fluidity. However, when temperature increases, it causes dehydration of PO and EO groups which is relatively rapid for the PO group compared to the EO group and hence leads to instability to the mixed micelles, That, in turn, reduces the aggregation due to the mixed micelle formation, and hence, fluidity increases and approaches the ideal behavior. On the other hand, the weak negative deviation in P103 + P123 mixtures at 25°C is again due to increased fluidity, but that reverts to ideal behavior as temperature increases and even shows positive deviation at higher temperatures. It means that the dehydration in P103 and P123 micelles happens to such an extent that both components start showing unfavorable mixing. It all happens due to the presence of a much larger number of PO units in both P103 and P123 which dehydrate rapidly as temperature increases and even loose solubility in the aqueous phase. This reduces the

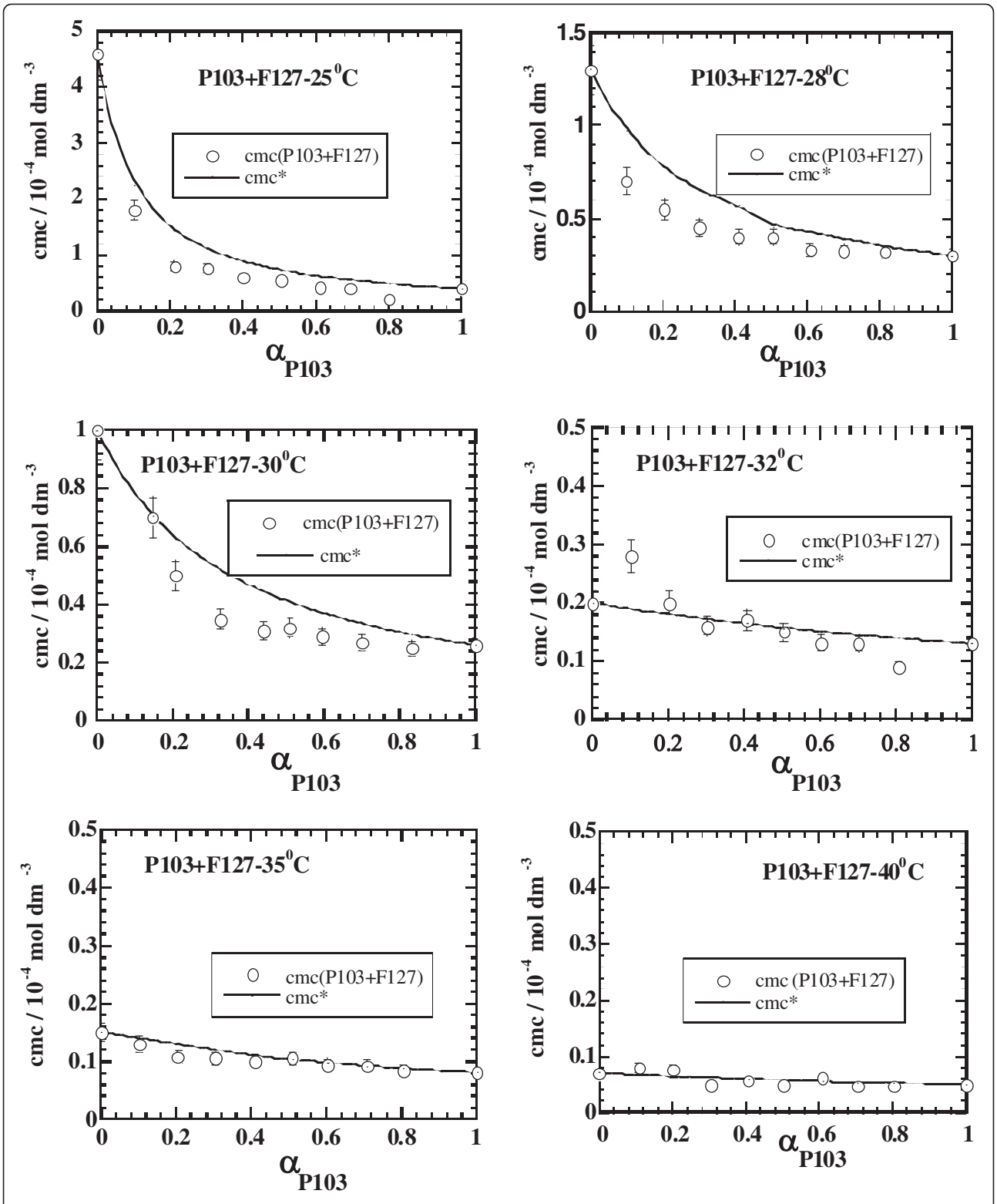

Figure 5 Plot of mixed CMC versus α_{P103} for P103 + F127 mixture at various temperatures. CMC* is the ideal CMC value.

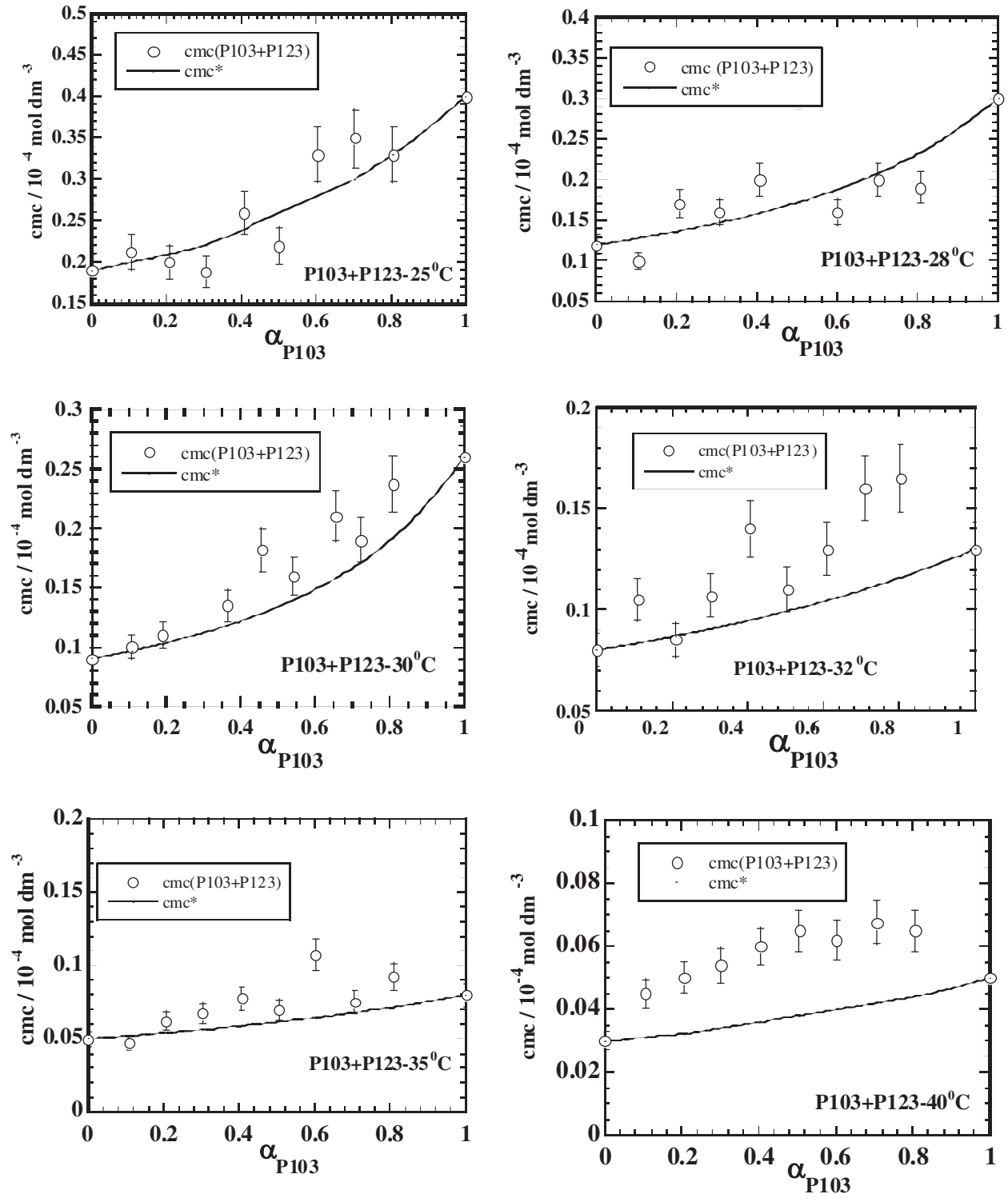

Figure 6 Plot of mixed CMC versus α_{P103} for P103 + P123 mixture at various temperatures. CMC* is the ideal CMC value.

micelle formation in each case, and hence, the system approaches the ideal behavior as temperature starts increasing but eventually reverts to positive deviations at a higher temperature due to decreased solubility.

Temperature effect can further be evaluated by computing the regular solution parameter β for each mixture at α_1 = 0.5 ($\beta_{0.5}$) (Figure 8). Both mixtures start with negative β values at 25°C, which become less negative

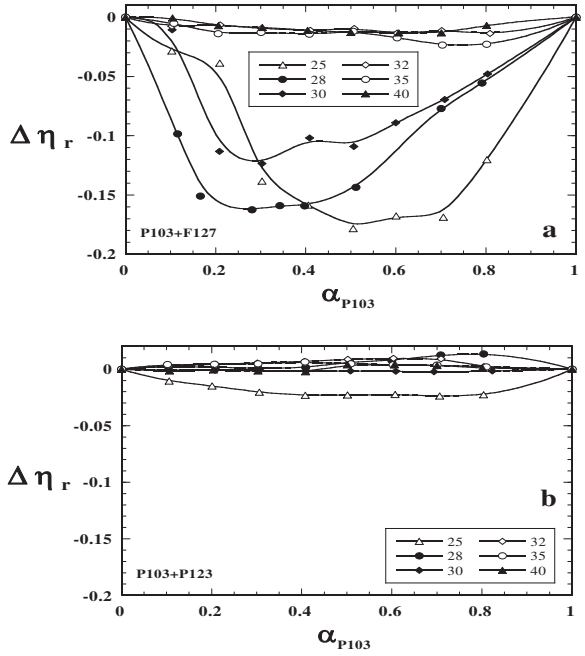

Figure 7 Plot of excess relative viscosity, $\Delta\eta_r$, versus α_{P103}. For (**a**) P103 + F127 and (**b**) P103 + P123 mixtures over the whole mole fraction range at different temperatures.

with the increase in temperature. The values remain negative from 25°C to 40°C for P103 + F127, while those for P103 + P123 change to positive somewhere close to 30°C. Within the framework of the regular solution theory, the negative β value is explained on the basis of attractive interactions between the unlike TBP components, while the positive value can be due to the unfavorable mixing. Thus, an increase in the temperature brings unfavorable mixing among both unlike TBP components in both kinds of mixed micelles. A greater

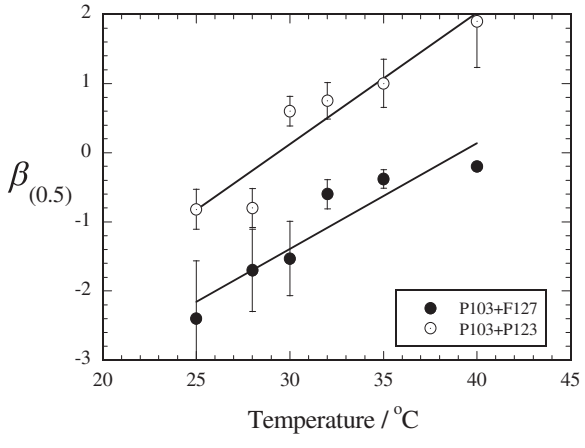

Figure 8 Plot of regular solution interaction parameter, $\beta_{(0.5)}$, versus temperature. For P103 + F127 and P103 + P123 mixtures at $\alpha_{P103} = 0.5$.

dehydration of PO groups in the case of P103 + P123 mixtures with greater number of PO units shows a stronger temperature effect, and that is why β shifts to a positive value at a much lower temperature around 30°C. Whereas, this is not happing over the whole temperature range studied in the case of P103 + F127 mixtures due to the presence of a relatively lesser number of PO groups. Although mixed micelle formation between two TBPs is governed by the predominantly hydrophobic interactions operating between the predominantly hydrophobic PPO domains of unlike TBPs, an increase in the temperature reduces their aqueous phase solubility and adversely affects the hydrophobic interactions responsible for the mixed micelle formation. That is why this effect is more prominent in the case of P103 + P123 mixtures with a larger PPO domain in comparison to that of P103 + F127.

Critical micelle temperature

TBPs are known to have micelle formation with respect to the variation of temperature, and the temperature where it happens is known as CMT, an analogous term used for this purpose to that of CMC where micelle formation occurs due to a change in concentration. CMT is considered to be having more relevance as far as their shelf life under varying temperatures is concerned because many industrial products in the cosmetic industry consist of more than one TBP component. Although, several studies have reported the CMT, little is known about the mixed CMT behavior. Experimental CMT values for some binary mixtures are shown in (Figure 9) along with the ideal mixing. In most cases, they show negative deviations from ideal behavior except in the case of P104 + P103 where the CMT values mainly lie close to that of the ideal behavior. A negative departure of CMT values indicates that the mixed micellization is taking place at lower temperatures and can be explained on the basis of favorable interactions between the unlike TBP components, and that shifts the mixed CMT to lower temperatures. Greater departure accounts for stronger interactions between the components of P103 + L64/P84 binary mixtures. The close-to-ideal mixing happening in the case of P104 $[(EO)_{18}(PO)_{58}(EO)_{18}]$ and P103 $[(EO)_{17}(PO)_{60}(EO)_{17}]$ is due to the little difference between the number of PO as well as EO units. This allows the unlike polymer macromolecule to accommodate in the mixed state without significant alterations in the overall hydrophilic or hydrophobic environment. On the contrary, this is not the case when L64 $[(EO)_{13}(PO)_{30}(EO)_{13}]$ and P84 $[(EO)_{19}(PO)_{43}(EO)_{19}]$ have been taken. In both these cases, there is a large difference in the PO units of these polymers compared with that of P103. Thus, in the event of mixed micelle formation, a larger PPO block of P103 has to accommodate with the

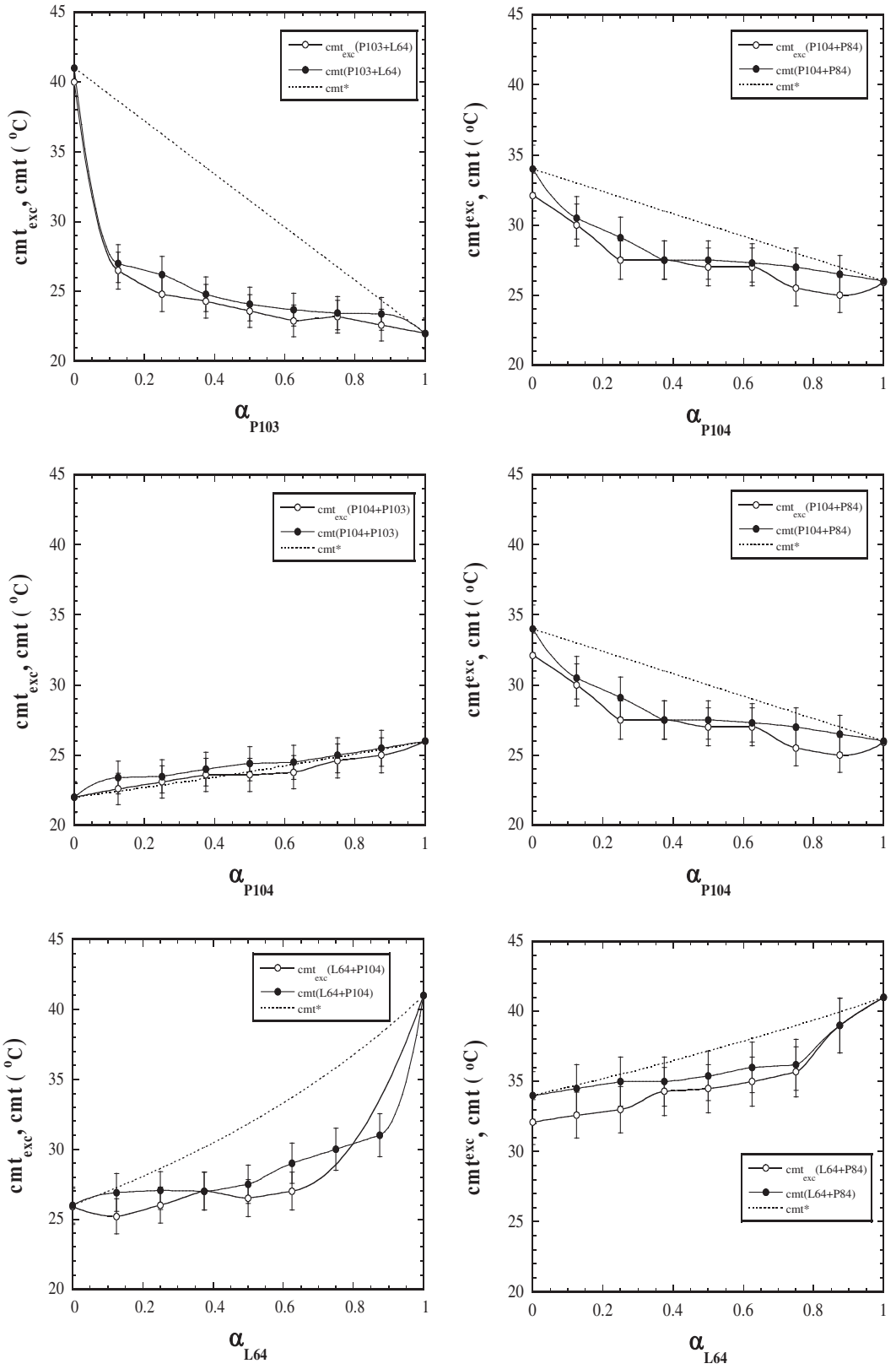

Figure 9 Plot of CMT and CMT_{exc}(°C) versus $\alpha_{P103,P104,L64}$. For P103 + L64, P103 + P84, P104 + P103, P104 + P84, L64 + P104, and L64 + P84 binary mixtures.

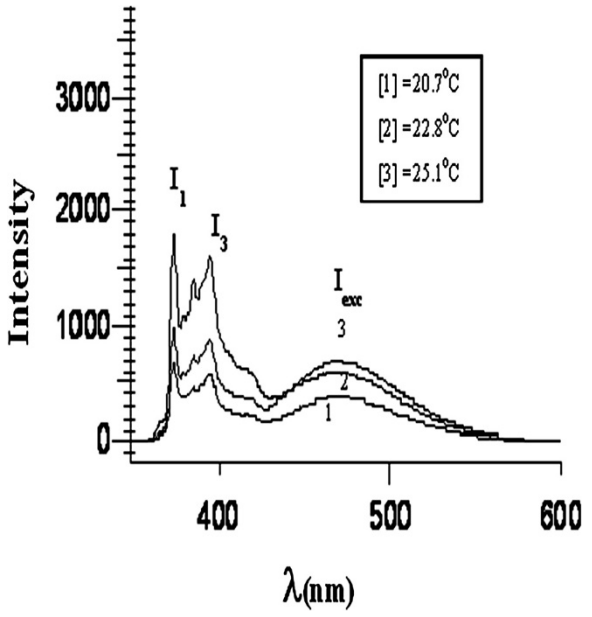

Figure 10 Pyrene emission spectrum at various temperatures of [P103] = 5.0 × 10^{-4} mol dm^{-3}. I_1, I_3, and I_{exc} are the intensities of the first, third, and excimer bands of pyrene.

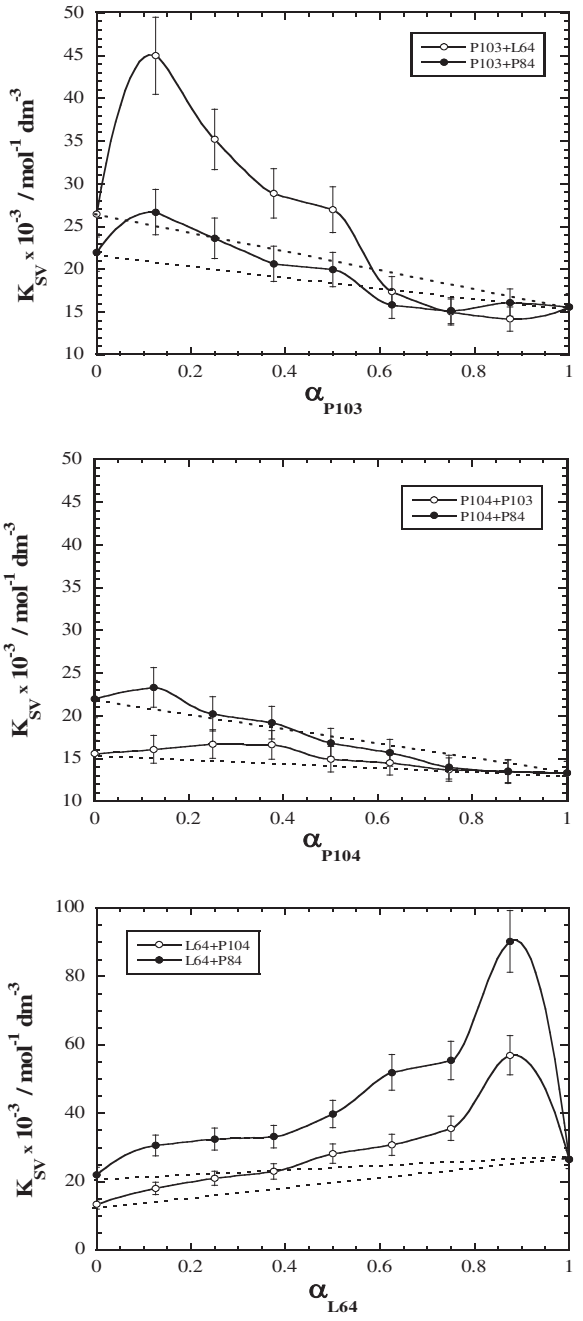

Figure 11 Plot of K_{SV} versus $\alpha_{P103/P104/L64}$. For P103 + L64/P84 binary mixtures, P104 + P103/P84 binary mixtures, and L64 + P104/P84 binary mixtures at 45°C.

shorter PPO block of either L64 or L84 in the core of the mixed micelle. This ensures the micelle transitions with greater compatibility among the components in the mixed state (Figure 9).

Quenching of pyrene by a suitable quencher (Q) such as hexadecylpyridinium chloride (HPyCl) under steady-state conditions can also be used to explain these results and assumed that the fluorescence lifetime of pyrene is longer than the residence time of the quencher in a micelle. A suitable [pyrene]/[mixed micelle] and [Q]/[mixed micelle] ratios ensure the Poisson distribution. The fluorescence intensity of the first vibronic band of (Figure 10) pyrene decreases with the increase in [Q] without the appearance of any new band (not shown). A Stern-Volmer relationship is used to calculate the collisional quenching constant, called the Stern-Volmer constant (K_{SV}) [99-102]. These K_{SV} values for various binary mixtures (Figure 11) vary nonlinearly with positive deviations from the ideality, which are predominant in the case of P103 + L64/P84, thus demonstrating that the quenching is facilitated in these mixtures. This can be attributed to the presence of a suitable solubilizing environment provided by the mixed micelles for an effective quenching to take place. The quenching is prominent in the L64/P84-rich region of the mixture which means that the small amount of the induction of P103 generates a favorable environment for the solubilization of both the quencher and pyrene. In the rich region of P103, the much larger micellar core with predominantly greater amount of PO units will make the encounters of both the quencher and pyrene difficult; as a result, quenching decreases.

The excimer emission is produced by the collisional quenching between the excited (Py^*) and ground state (Py) monomers of the fluorescence probe. Thus, the

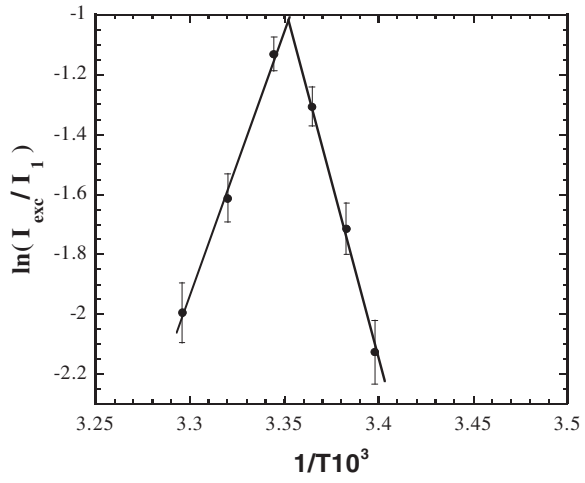

Figure 12 Plot of $\ln(I_{exc}/I_1)$ versus $1/T$ for pure P104 at [P104] = 5.0 × 10^{-4} mol dm^{-3}.

mechanism of the excimer dimer (D^*) formation can be written in the following way:

$$Py^* + Py \underset{k_{ED}}{\overset{k_{EF}}{\rightleftharpoons}} D^* \quad (1)$$

$$Py^* \xrightarrow{k_{MF}} Py + hv \quad (2)$$

$$D^* \xrightarrow{k_{DF}} 2Py + hv, \quad (3)$$

where k_{EF}, k_{ED}, k_{MF}, and k_{DF} are the constants of excimer formation, excimer dissociation, monomer fluorescence, and dimer fluorescence, respectively. The kinetics of excimer formation can further be explained under two sets of experimental conditions, i.e., low-temperature and high-temperature behaviors within the temperature range studied herein. At low temperature, I_{exc}/I_1 ratio can be written as:

$$\frac{I_e}{I_1} = \frac{k^1{}_{EF}[Py]}{k_{MF}} \exp\left[{}^{-}W_{EF}/_{kT}\right], \quad (4)$$

where k^1_{EF} and W_{EF} are the frequency factor (limiting value of k^1_{EF} as $T \infty$) and activation energy of excimer formation, respectively, and k is Boltzmann's constant. Similarly, at high temperature, the I_{exc}/I_1 ratio is given by:

$$\frac{I_e}{I_1} = \frac{k_{DF}k^1{}_{EF}[Py]}{k^1{}_{ED}k_{MF}} \exp\left[{}^{B}/_{kT}\right], \quad (5)$$

where B is the excimer binding energy = $W_{ED} - W_{EF}$, and k^1_{EF} is the frequency factor. Equations 4 and 5 suggest that $\ln(I_{exc}/I_1)$ shows an increase and decrease linearly with $1/T$, respectively, at fixed [Py]. Figure 12 shows such a variation for P104 at different temperatures. Here, an intersection of two linear lines gives the CMT 26°C. Hence, the kinetics of pyrene solubilization in TBP micelles can be analyzed within two different sets of experimental conditions, one is below and the other above 26°C. The former gives the activation energy for the excimer formation (Figure 13), while the latter gives the binding energy (Figure 14) between Py* and Py.

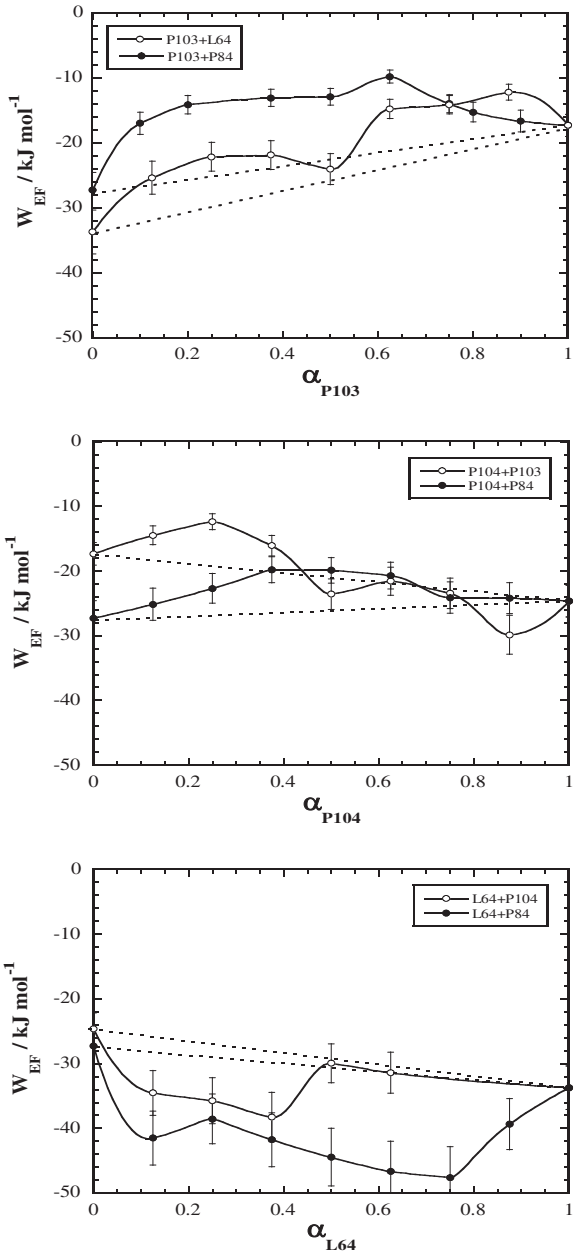

Figure 13 Plot of energy of activation (W_{EF}) of the pyrene probe for the excimer formation versus $\alpha_{P103/P104/L64}$. For P103 + L64/P84 binary mixtures, P104 + P103/P84 binary mixture, and L64 + P104/P84 binary mixtures.

Figure 13 shows the variation of W_{EF} over the whole mole fraction range for all mixtures. These values for P103 + L64/P84 (Figure 13, top) show a positive deviation from the ideal mixing (shown by dotted lines),

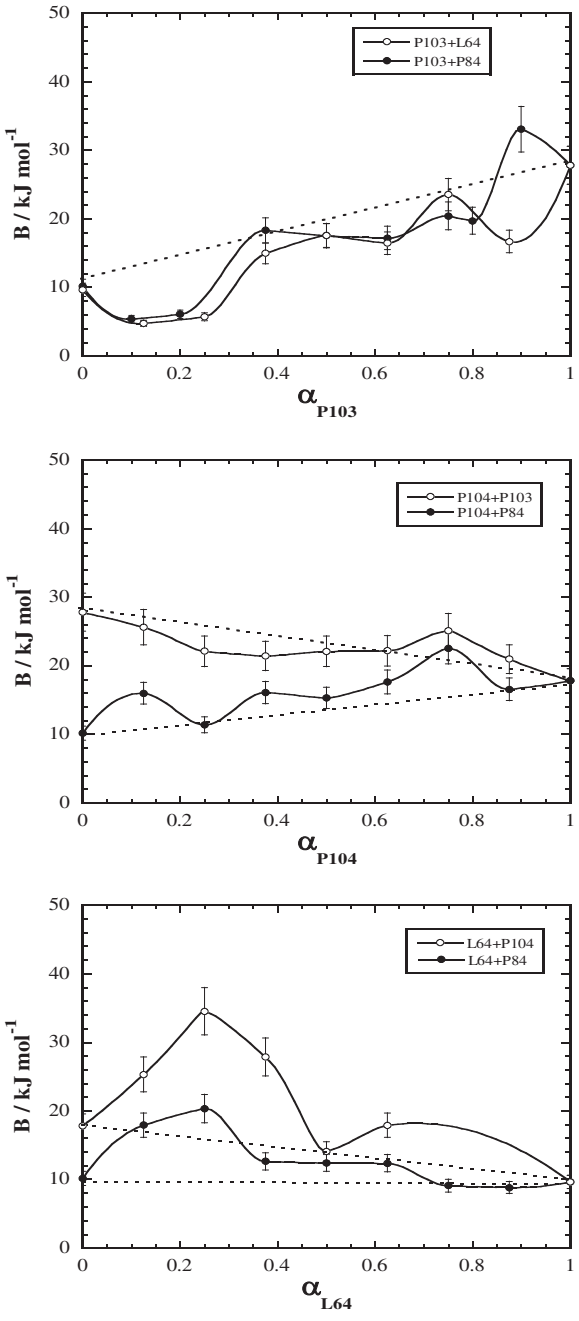

Figure 14 Plot of binding energy (*B*) of the pyrene probe for the excimer formation versus $\alpha_{P103/P104/L64}$. For P103 + L64/P84 binary mixtures, P104 + P103/P84 binary mixture, and L64 + P104/P84 binary mixtures.

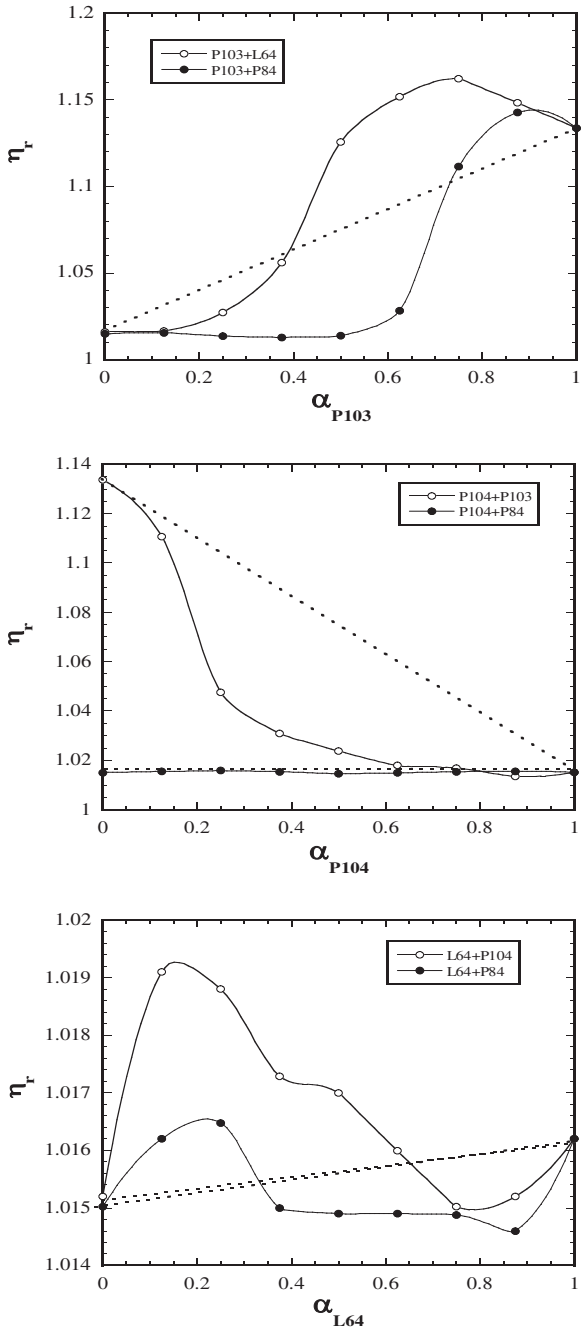

Figure 15 Plot of η_r versus $\alpha_{P103/P104/L64}$. For P103 + L64/P84 binary mixtures, P104 + P103/P84 binary mixtures, and L64 + P104/P84 binary mixtures at 45°C.

while those for P104 + P103/P84 (Figure 13, middle) remain mostly close to the ideal behavior. Figure 13 (bottom) shows negative deviations in W_{EF} values from ideality for L64 + P104/P84 mixtures. A decrease in the W_{EF} values at all mole fractions of P103 + L64/P84 can be attributed to the facilitation of the excimer formation which is also evident from the higher K_{SV} values for these mixtures. These results can also be related to the relative viscosity (η_r) behavior for these mixtures (Figure 15). A smaller η_r value than the ideal behavior especially in the P103-poor region of the mixtures shows the attractive interactions between the components that might be responsible for lower W_{EF} in comparison to their pure states. This is further supported by the negative

deviations in B values from the ideal behavior (Figure 14, top). The variation in the B values for these mixtures (Figure 14, middle) fully supports this fact. The η_r of P104 + P84 mixtures (Figure 15, middle) shows clear ideal mixing, but the negative deviation in the case of P104 + P103 is due to unknown reasons. An increase in the W_{EF} value for L64 + P103/P84 mixtures (Figure 13, bottom) from their pure components clearly indicates the reduction in excimer formation. This is again complimentary with the positive deviations in the B values from the corresponding ideal mixing (Figure 14, bottom). Both figures demonstrate that the variation in W_{EF} and B values is mainly predominant in the L64-poor regions of both mixtures. The positive deviations in the η_r (Figure 15, bottom) from the ideal behavior especially in the L64-poor region further confirm these results.

The variation of all the micellar parameters and photophysical properties indicates that the mixed micelles between the components of P103 + L64 and P103 + P84 mixtures form due to attractive interactions. These interactions arise from the mutual compatible arrangement among the unlike TBP monomers in the mixed state in such a way that steric hindrances are minimized. On the other hand, mixtures of P104 + P103 and P104 + P84 prefer to remain ideal in their mixed state, while the mixtures of L64 + P104 and L64 + P84 show mainly unfavorable mixing.

Applications

Solubilization and drug delivery agents

The low solubility in biological fluids displayed by about 50% of the drugs still remains the main limitation in oral, parenteral, and transdermal administration. To overcome these drawbacks, inclusion of hydrophobic drugs into polymeric micelles is one of the most attractive alternatives. Amphiphilic poly(ethylene oxide)-poly(propylene oxide) block copolymers are thermoresponsive materials that display unique aggregation properties in aqueous medium. Due to their ability to form stable micellar systems in water, these materials are broadly studied as hydrosolubilizers for poorly water-soluble drugs. This occurs because the core of the micelle provides a hydrophobic microenvironment, suitable for solubilizing such molecules. The phenomenon of solubilization forms the basis for many practical applications of amphiphiles. The most important applications of PEO-PPO-based copolymers in the pharmaceutical technology field are for attaining improved solubility, stability, release, and bioavailability of drugs [103]. Hydrophobic Pluronic block copolymers (PBC) form lamellar aggregates with a higher solubilization capacity than spherical micelles formed by hydrophilic PBC. However, they also have a larger size and low stability. To overcome these limitations, Kabanov et al. [104] prepared binary mixtures from hydrophobic PBC (L121, L101, L81, and L61) and hydrophilic PBC (F127, P105, F87, P85, and F68). In most cases, PBC mixtures were not stable, revealing formation of large aggregates and phase separation within 1 to 2 days. However, stable aqueous dispersions of the particles were obtained upon (1) sonication of the PBC mixtures for 1 or 2 min or (2) heating at 70°C for 30 min. It was observed that among all combinations, L121/F127 mixtures (1:1% weight ratio) formed stable dispersions with a small particle size. The solubilizing capacity of this system was examined using a model water-insoluble dye, Sudan (III). Mixed L121/F127 aggregates exhibited approximately tenfold higher solubilization capacity compared to that of F127 micelles. Thus, stable aqueous dispersions of nanoscale size were prepared from mixtures of hydrophobic and hydrophilic PBC by using the external input of energy. The prepared mixed aggregates can efficiently incorporate hydrophobic compounds. To enhance stability of micelles in the blood stream upon dilution, Pluronic L121 micelles were cross-linked through their hydrophilic shells [105]. To form the cross-links, the end hydroxyl groups of Pluronic L121 were first chemically converted to aldehydes and then bridged via Schiff bases. This greatly reduced the CMC of the micelles and enhanced the micelle stability. A series of studies used Pluronic P105 micelles for the delivery of Dox into solid tumors in mice [106-109]. In these studies, the localized ultrasonic irradiation of the tumor was applied upon accumulation of the micelles in the tumor interstitium to facilitate the drug release into the tumor cells [108]. Furthermore, the ultrasound-enhanced intracellular uptake of Dox administered with the Pluronic P105 micelles was demonstrated *in vitro* [106]. It was suggested that the enhanced uptake was caused by either micelle disintegration that released free Dox or cell membrane perturbations that facilitated the cellular uptake of the micelles as a whole. Overall, micellar delivery combined with ultrasonic irradiation resulted in a substantial decrease of the tumor growth rates compared to a positive control.

Nano drug delivery

Polymer nanomaterials have sparked a considerable interest as vehicles used for diagnostic and therapeutic agents; research in nanomedicine has not only become a frontier movement but is also a revolutionizing drug delivery field. A common approach for building a drug delivery system is to incorporate the drug within the nanocarrier that results in increased solubility, metabolic stability, and improved circulation time. The recent developments indicate that select polymer nanomaterials can implement more than only inert carrier functions by being biological response modifiers. The Pluronic block copolymers cause various functional alterations in cells. The key

attribute for the biological activity of Pluronics is their ability to incorporate into membranes followed by subsequent translocation into the cells and affecting various cellular functions, such as mitochondrial respiration, ATP synthesis, activity of drug efflux transporters, apoptotic signal transduction, and gene expression. As a result, Pluronics cause drastic sensitization of MDR tumors to various anticancer agents, enhance drug transport across the blood-brain and intestinal barriers, and cause transcriptional activation of gene expression both *in vitro* and *in vivo*. Pluronics have a broad spectrum of biological response-modifying activities which make it one of the most potent drug targeting systems available, resulting in a remarkable impact on the emergent field of nanomedicine. Incorporation of low molecular mass drugs into Pluronic micelles can increase drug solubility and drug stability and can improve drug pharmacokinetics and biodistribution. Polymeric micelles were utilized for delivery of CNS drugs across the blood-brain barrier [110,111], oral delivery of drugs [112-114], and tumor-specific delivery of antineoplastic agents [115-117]. For example, neuroleptic drug-loaded Pluronic P85 micelles were targeted to the brain by conjugating the micelles with neurospecific antibodies or insulin as targeting moieties [118]. An improvement of oral bioavailability of a poorly water-soluble phytoestrogen, genistein, was achieved by incorporation of this drug into Pluronic F127 micelles [117]. Pluronic block copolymers were also reported to significantly enhance the bioavailability of various antibacterial and antifungal drugs and to enhance the activity of these drugs with respect to many microorganisms [119-122]. Lee et al. [123] developed a binary mixing system with two Pluronics, L121/P123, as a nanosized drug delivery carrier. The lamellar-forming Pluronic L121 (0.1 wt.%) was incorporated with Pluronic P123 to produce nanosized dispersions (in the case of 0.1 and 0.5 wt.% P123) with high stability due to Pluronic P123 and high solubilization capacity due to Pluronic L121. The binary systems were spherical and less than 200 nm in diameter, with high thermodynamic stability (at least 2 weeks) in aqueous solution. The CMC of the binary system was located in the middle of the CMC of each polymer. In particular, the solubilization capacity of the binary system (0.1/0.1 wt.%) was higher than mono-systems of P123. The main advantage of binary systems is overcoming limitations of mono-systems to allow tailored mixing of block copolymers with different physicochemical characteristics. Kadam et al. [124] investigated the effect of the molecular characteristics of EO-PO triblock copolymers Pluronic P103 ($EO_{17}PO_{60}PEO_{17}$), P123 ($EO_{19}PO_{69}EO_{19}$), and F127 ($EO_{100}PO_{65}EO_{100}$) on micellar behavior and solubilization of a diuretic drug, hydrochlorothiazide (HCT). The CMTs and size for empty as well as drug-loaded micelles are reported. The CMTs and micelle size depended on the hydrophobicity and molecular weight of the copolymer; a decrease in CMT and increase in size were observed on solubilization. The solubilization of the drug HCT in the block copolymer nanoaggregates at different temperatures (28°C, 37°C, 45°C) and pH (3.7, 5.0, 6.7) and in the presence of added salt (NaCl) was monitored by using UV-vis spectroscopy, and solubility data were used to calculate the solubilization characteristics: micelle-water partition coefficient (P) and thermodynamic parameters of solubilization *viz.* Gibbs free energy (ΔG_s°), enthalpy (ΔH_s°), and entropy (ΔS_s°). It is observed that the solubility of the drug in the copolymer increases with the trend: P103 > P123 > F127. The solubilized drug decreased the cloud point (C_P) of copolymers. Results showed that the drug solubility increases in the presence of salt but significantly enhances with the increase in the temperature and at a lower pH in which the drug remains in the nonionized form.

Synthesis of gold nanoparticles

Gold nanoparticles are a great deal of recent interest in the context of emerging nanotechnology applications. At the nanoscale, they exhibit unique quantum and surface properties, different from those of atoms as well as bulk materials [125-128]. Depending on the applications they are being synthesized for, they can be synthesized in many different ways. One of the easiest and convenient ways is the chemical reduction method which involves the use of four basic materials, namely, solvent, metal salt, reducing agent, and stabilizing agent [129-131]. Recently, the use of block copolymers for the synthesis of gold nanoparticles is found to have many advantages; for example, a block copolymer not only plays the dual role of reductant and stabilizer but also provides an economical and environmentally benign way for the synthesis of gold nanoparticles [132-134]. The hydrophobic blocks of the block copolymers (PPO) form the core of these micellar aggregates, whereas the hydrophilic ones (PEO), with the surrounding water molecules, form the corona. The block copolymers can be used to produce metal nanoparticles because of their ability to reduce metal ions. On mixing the aqueous solution of metal (e.g., gold) salt and block copolymers, these polymeric nanostructured matrixes engulf the ionic metal precursors, which after subsequent reduction form nanoparticles. Self-assembly of a block copolymer in this method is utilized to control the synthesis of gold nanoparticles [135]. The formation of gold nanoparticles from $AuCl_4^-$ comprises three main steps: reduction of $AuCl_4^-$ ions by the block copolymers in the solution and formation of gold clusters, adsorption of block copolymers on gold clusters and reduction of $AuCl_4^-$ ions on the surfaces of these gold clusters, and growth of gold particles in steps and finally its stabilization by block copolymers [136]. The role of block copolymers in the synthesis (formation rate, yield, stability, shape, and size of

nanoparticles) varies with their molecular weight, PEO/PPO block length, polymer concentration, and temperature [137-139]. The formation of high-concentration gold nanoparticles at room temperature is reported in the block copolymer-mediated synthesis where the nanoparticles have been synthesized from hydrogen tetrachloroaureate (III) hydrate ($HAuCl_4.3H_2O$) using block copolymer P85 ($EO_{26}PO_{39}EO_{26}$) in aqueous solution [140]. The formation of gold nanoparticles in these systems has been characterized using UV-visible spectroscopy and SANS. It showed that the presence of an additional reductant (trisodium citrate) can enhance nanoparticle concentration by manyfold, which does not work in the absence of either of these (additional reductant and block copolymer). Bakshi et al. [141] used aqueous micellar solutions of F68 (PEO_{78}-PPO_{30}-PEO_{78}) and P103 (PEO_{17}-PPO_{60}-PEO_{17}) triblock polymers to synthesize gold (Au) nanoparticles at different temperatures. They observed that all reactions were carried out with the PEO-PPO-PEO micellar surface cavities present at the micelle-solution interface and were precisely controlled by the micellar assemblies. Marked differences were detected when predominantly hydrophilic F68 and hydrophobic P103 micelles were employed to conduct the reactions, and the presence of well-defined predominantly hydrophobic micelles with a compact micelle-solution interfacial arrangement of surface cavities ultimately controlled the reaction.

Mesomorphous behavior

Numerous investigations of the behavior of PEO-PPO-PEO triblock copolymers in aqueous solutions and the adsorption of these copolymers at solid-liquid interfaces were carried out in the past decades [31,52,142]. Also, since the aggregated structure of PEO-PPO-PEO triblock copolymers is controlled depending on temperature, concentration, and the addition of additives, they have been used as structure-directing organic materials for the synthesis of inorganic materials with a controlled size, shape and structure. Bagshaw et al. prepared mesoporous silica molecular sieves using nonionic polyethylene oxide surfactants in a neutral condition [143]. The hydrogen bonding between the hydrophilic part of polymers and the inorganic precursor followed by molecular rearrangement involving the amphiphilic nature of polymers was the key factor for the preparation of this material. Zhao et al. reported on the synthesis of mesoporous silica structures using nonionic alkyl poly(oxyethylene) surfactants and poly(alkylene oxide) block copolymers in an acid media, which included cubic, three-dimensional hexagonal, two-dimensional hexagonal, and lamellar mesostructures [144]. Kim et al. developed an economical and simple method for the preparation of sub-micrometer hematite particles with a narrow size distribution and an isotropic shape. To obtain hematite particles, the ferric ion solution was aged at an elevated temperature in the presence of poly(ethylene oxide)-block-poly(propylene oxide)-block-poly(ethylene oxide) (PEO-PPO-PEO) triblock copolymer EO20PO70EO20 (P123). The resulting particles also show a disordered mesoporous structure and retain their shape after calcinations [145]. Huang et al. synthesized a series of highly ordered mesoporous carbonaceous frameworks with diverse symmetries by using phenolic resols as a carbon precursor and mixed amphiphilic surfactants of poly (ethylene oxide)-*b*-poly(propylene oxide)-*b*-poly(ethylene oxide) (PEO-PPO-PEO) and reverse PPO-PEO-PPO as templates by the strategy of evaporation-induced organic-organic self-assembly [146]. The blends of block copolymers can interact with resol precursors and tend to self-assemble into cross-linking micellar structures during the solvent evaporation process, which provides a suitable template for the construction of mesostructures. An understanding of the organic-organic self-assembly behavior in the mixed amphiphilic surfactant system would pave the way for the synthesis of mesoporous materials with controllable structures.

Other applications

Cobalt determination

da Silva et al. [147] proposed a new method for Co(II) determination based on the use of the triblock copolymer as micellar medium instead of chloroform. The proposed strategy is environmental friendly because the copolymer is biodegradable and nontoxic. The method is based on the formation of a cobalt-1-nitroso-2-naphthol complex in the micellar triblock copolymer compound solution constituted by PEO and PPO. Experimental conditions such as pH, the molecular weight, and the PEO/PPO ratio of the triblock copolymer were optimized. Results obtained for cobalt determination in vitamins with this novel method showed excellent agreement with those obtained using atomic absorption spectrometry.

Boundary lubrication

Lubricants most commonly used in textile manufacturing are composed of fatty acids, mineral oils, ethoxylated acids, and silicones. Poly(oxyethylene)-poly(oxypropylene)-poly (oxyethylene) (PEO-PPO-PEO; Pluronic) triblock copolymers have been of great interest as lubricants due to their numerous advantages, including good solubility in water and organic solvents, compatibility with most surfactants, and availability as electrolyte-free material. The molecular weight and the PEO/PPO ratio of these surfactants can be adjusted to tailor their properties as lubricants, texturizers, softeners, emulsifiers, dispersers, and antistatic and wetting agents. Pluronic copolymers have high wetting and spreading ability, allowing them to form uniform coatings on textiles that can result in

low friction, antistatic properties, dye-leveling improvement, and easy cleaning. Li et al. [148] studied lubrication behavior of an aqueous solution of PEO-PPO-PEO symmetric triblock copolymer on thin films of polypropylene (PP), polyethylene (PE), and cellulose. It was observed that the friction coefficient on PP and PE was reduced after adsorption from the PEO-PPO-PEO aqueous solution, while the opposite effect was observed for cellulose surfaces. XPS was used to verify the presence of the lubricant on the polymeric substrates and to evaluate its removal by water washing. The lubricant layer was easily removed with water from the PP and cellulose surfaces, while a durable layer was found on PE.

As membrane material for intermediate-temperature DMFCs

Triblock copolymer/Nafion blend membranes (DuPont, Wilmington, DE, USA) facilitate proton conduction in direct methanol fuel cells (DMFCs) at intermediate temperatures. Hu et al. [149] investigated the interaction between the two polymer components by FT-IR spectroscopy. The blend membranes show higher proton conductivity than recast Nafion under partially anhydrous conditions. Protons can be transported with the assistance of an ether chain under such conditions at elevated temperature. In addition, the membranes exhibit more favorable methanol permeability and selectivity. This kind of blend membrane shows somewhat better performance in DMFC compared to bare recast Nafion at intermediate temperature (≥120°C). This helps to design membrane materials with enhanced proton conductivity under conditions typical of intermediate-temperature DMFCs.

Conclusions

Mixed micelle parameters of different TBPs mixtures are discussed. It has been observed that synergistic mixing is governed by the compatibility between the different blocks of PEO units of different TBPs. A large difference between the PPO and PEO blocks of different polymers leads to the unfavorable mixing. These findings help us to further explore the industrial applications of such TBPs.

Competing interests

The authors declare that they have no competing interests.

Authors' contributions

VS collected the references for this work and did additional studies and calculations. Part of this work is related to the Ph.D. thesis of NK. PK compiled and wrote the review along with PND. All authors read and approved the final manuscript.

Acknowledgments

PK acknowledges the financial assistance from the DST (Ref #SERB/F/0328/2012-13) project.

Author details

[1]Department of Chemistry, KSKV Kachchh University, Bhuj, Gujarat 370001, India. [2]Department of Chemistry, B.B.K. D.A.V. College for Women, Amritsar, Punjab 143005, India. [3]Department of Chemistry, Lyallpur Khalsa College, Jallandhar, (Punjab) 144001, India.

Received: 1 November 2012 Accepted: 17 December 2012
Published: 12 February 2013

References

1. Schmolka IR (1984) Cosmetics and Toiletries 99:69
2. Bahadur P, Resis G (1991) Tenside Cloud Surf Deter 28:173
3. Alexandridis P, Olsson U, Lindmann B (1998) Langumir 14:2627
4. Parsipany NJ (1989) Pluronic and tetronic surfactants, technical brochure. BASF-Corporation, New Jersey
5. Janert PK, Schick M (1997) Macromolecules 30:137
6. Janert PK, Schick M (1998) Macromolecules 31:1109
7. Alexandridis P (1998) Macromolecules 31:6935
8. Alexandridis P, Hatton TA (1995) Colloids Surf A 96:1
9. Groot RD, Madden TJ (1998) J Chem Phys 108:8713
10. Burger C, Micha MA, Oerstreich S, Foster S, Anntonietti M (1998) Europhys Lett 42:425
11. Liu T, Wu C, Xie Y, Liang D, Zhou S, Nace VM, Chu B (2000) ACS Symp Ser 765:2
12. Edens MW (1996) Surf Sci Series 60:185
13. Alexandridis P (1996) Curr Opin J Colliodal and Interface Sci 1:490
14. Yokoyama M (1992) Crit Rev Therapeutic Drug Carrier Systems 9:213
15. Guzman M, Garica FF, Molpeceres J, Aberturas MR (1992) Int J Pharm 80:119
16. Murhammer DW, Goochee CF (1990) Biotechnol Prog 6:391
17. Harris JM, Zalpisky S (1997) Poly(ethylene glycol): chemistry and biological application. American Chemical Society, Washington, DC
18. Tedder DW, Pohland FG (1990) Emerging technologies in hazardous waste management. American Chemical Society, Washington, DC
19. Rodriguez SC, Singer EJ (1996) Surf Sci Series 20:211
20. Zallipsky S (1995) Bioconjugate Chem 6:150
21. Torchilin VP, Truketskey VS, Whiteman KR, Caliceti P, Ferruti P, Veronesi FM (1995) J Pharm Sci 84:1049
22. Schmolka IR (1997) J Am Oil Chem Soc 54:110
23. Mura JL, Reiss G (1995) Polym Adv Technol 6:497
24. Forster S, Antonietti M (1998) Adv Mater 10:4195
25. Caruso RA, Giersbig M, Willig F, Antonietti M (1998) Ber Bunsen-Ges Phys Chem 102:1540
26. Chander S, Polat H, Mohal B (1995) Trans Soc Min Metall Explor 296:55
27. Lindmann B, Wennerstorm H (1980) Topics of current chemistry. Springer, Berlin, p 87
28. Rices G, Bahadur P, Hurtez G (1985) Block copolymers. In: Mark HF, Kroschwitz J (ed) Encyclopedia on polymer science and engineering, 2nd edition. Wiley, New York, p 314
29. Alexandridis P, Holzwarth JF, Hatton TA (1994) Macromolecules 27:2414
30. Cau F, Lacelle S (1996) Macromolecules 29:170
31. Yang L, Alexandridis P, Steyler DC, Kositza MJ, Holzwarth JF (2000) Langmuir 16:8555
32. Hunter RJ (1987) Foundations of colloid science. Oxford University Press, New York, pp 1–565
33. Thurn T, Couderc S, Sidhu J, Bloor DM, Penfold J, Holzwarth JF, Wyn-Jones E (2002) Langmuir 18:9267
34. Bakshi MS, Kaura A, Kaur G (2006) J Colloid and Interface Science 296:370
35. Bakshi MS, Kaura A, Mahajan RK (2005) Colloids Surf A 262:168
36. Bakshi MS, Sharma P, Kaur G, Sachar S, Banipal TS (2006) Colloids Surf A 278:218
37. Bakshi MS, Sachar S (2006) Colloids Surf A 276:146
38. Bakshi MS, Sachar S (2006) J Colloid Interface Sci 296:309
39. Mahajan RK, Kaur N, Bakshi MS (2005) Colloids Surf A 255:33
40. Bakshi MS, Singh J, Kaur G (2005) Antagonistic mixing behavior of catonic Gemini surfactant and triblock polymers in mixed micelle. J Colloid Interface Sci 285:403
41. Bakshi MS, Kaur N, Mahajan RK (2006) Photochem Photobiol 183:146
42. Mahajan RK, Kaur N, Bakshi MS (2006) Colloids Surf A 276:221
43. Solan SL, Phillips RJ, Cotts PM, Dungan SR (1997) J Colloid Interface Sci 191:291
44. Holland RJ, Parker EJ, Guiney K, Zeld FR (1995) J Phys Chem 99:11981
45. Nakashima K, Anzai T, Fujimoto Y (1994) Langmuir 10:658
46. Almgren M, Bahadur P, Jannson M, Li P, Brown W, Bahadur A (1992) J Colloid Interface Sci 15:1157
47. Williams RK, Simard MA, Jolicoeur C (1985) J Phys Chem 89:178
48. Wen XG, Verrall RE (1997) J Colloid Interface Sci 196:215

49. Goldmints I, Von Gottberg FK, Smith KA, Hatton TA (1997) Langmuir 13:3659
50. Goldmints I, Holzwarth JF, Smith KA, Hatton TA (1997) Langmuir 13:6130
51. Malmsten M, Lindman B (1992) Macromolecules 25:5440
52. Wu C, Liu T, Chu B, Schneider DK, Fraziano V (1997) Macromolecules 30:4574
53. Wanka G, Hoffman H, Ulbricht W (1994) Macromolecules 27:4145
54. Alexandridis P, Nivaggioli T, Hatton TA (1995) Langmuir 11:1468
55. Prud'homme RK, Wu G, Schneider DK (1996) Langmuir 12:4651
56. Alexandridis P, Athanassiou V, Fukuda S, Hatton TA (1994) Langmuir 10:2604
57. Alexandridis P, Holzwarth JF (2000) Curr Opin J Colloid and Interface Sci 5:312
58. Almgren M, Brown W, Hvidt S (1995) Colloid Polym Sci 273:2
59. Mortensen K, Pedersen JS (1993) Macromolecules 26:805
60. Hecht E, Hoffmann H (1995) Colloids Surf A 96:181
61. Goldmints I, Yu GE, Booth C, Smith KA, Hatton TA (1999) Langmuir 15:1651
62. Genz A, Holzwarth JF (1986) Eur Biophys 13:323
63. Kositza MJ, Bohne C, Alexandridis P, Hatton TA, Holzwarth JF (1999) Macromolecules 32:5539
64. Zhou Z, Chu B (1988) J Colloid Interface Sci 126:171
65. Alasden AA, Whatley TL, Florence AT (1982) J Colloid Interface Sci 90:303
66. Attwood D, Collett JH, Tail CJ (1985) Int J Pharm 26:25
67. Zhou Z, Chu B (1988) Macromolecules 21:2548
68. Almgren M, Alisns J, Bahadur P (1991) Langmuir 7:446
69. Tontisakis A, Hilfiker R, Chu B (1992) J Colloid Interface Sci 135:427
70. Wanka G, Hoffman H, Ulbricht W (1990) Colloid Polym Sci 268:101
71. Brown W, Schillen K, Almgren M, Hvidt S, Bahadur P (1991) J Phys Chem 95:1850
72. Chu B, Zhou Z (1996) Surf Sci Ser 60:67
73. Sedev R, Steitz R, Findenegg GH (2002) Physica B 315:267
74. Alexandridis P, Chu D, Khan A (1996) Langmuir 12:2696
75. Alexandridis P, Olsson U, Lindmann B (1997) Langmuir 13:23
76. Mao G, Sukumaran S, Beaucage G, Sabougni ML, Thyagarajein P (2001) Macromolecules 34:552
77. Mitchell DJ, Tiddy GJT, Waring L, Bostock T, MacDonald M (1983) Chem Soc Farady Trans 1 79:975
78. Lawrence MJ (1990) Chem Soc Rev 90:753
79. Zhang L, Eisenberg A (1995) Science (Washington, DC) 268:1728
80. Gao Z, Varshney SK, Wong S, Eisenberg A (1994) Macromolecules 27:7923
81. Shen HW, Zhang LF, Eisenberg A (1999) J Am Chem Soc 121:2728
82. Desbaumes L, Eisenberg A (1999) Langmuir 15:36
83. Zhang LF, Yu K, Eisenberg A (1996) Science 272:1777
84. Zhang LF, Eisenberg A (1996) J Am Chem Soc 118:3168
85. Discher DE, Eisenberg A (2002) Science 297:967
86. Zhang LF, Bartels C, Yu YS, Shen HW, Eisenberg A (1997) Phys Rev Lett 79:5034
87. Talingting MR, Munk P, Webber SE (1999) Macromolecules 32:1593
88. Riegel IC, Eisenberg A (2002) Langmuir 18:3358
89. Yu K, Zhang LF, Eisenberg A (1996) Langmuir 12:5980
90. Cameron NS, Corbierre MK, Eisenberg A (1999) Can J Chem 77:1311
91. Yu G, Eisenberg A (1998) Macromolecules 31:5546
92. Yu YS, Zhang LF, Eisenberg A (1997) Langmuir 13:2578
93. Kindt JT (2002) J Phys Chem B 106:8223
94. van der Schoot P, Wittmer JP (1999) Linear aggregation revisited: rods, rings and worms. Macromol Theory Simul 8:428
95. Wittmer JP, van der Schoot P, Milchev A, Barrat JL (2000) J Chem Phys 113:6992
96. Hu J, Odom TW, Lieber CM (1999) Acc Chem Res 32:435
97. Han YJ, Kim JM, Stucky GD (2000) Chem Mater 12:2068
98. Booth C, Attwood D (2000) Macromol Rapid Commun 21:501
99. Stern O, Volmer M (1990) Phys Z 20:18
100. Wellar A (1976) Prog React Kinet 1:3246
101. Efthik MR, Gheron CA (1976) J Phys Chem 80:486
102. Gorner H, Stammel C, Mattey J (1997) J Photochem Photobiol A: Chem 120:171
103. Chiappetta DA, Sosnik A (2007) Eur J Pharm Biopharm 66:303
104. Oh KT, Bronich TK, Kabanov AV (2004) J Control Release 94:411
105. Yang TF, Chen CN, Chen MC, Lai CH, Liang HF, Sung HW (2007) Biomaterials 28:725
106. Gao Z, Fain HD, Rapoport N (2004) Mol Pharm 1:317
107. Gao ZG, Fain HD, Rapoport N (2005) J Control Release 102:203
108. Rapoport NY, Christensen DA, Fain HD, Barrows L, Gao Z (2004) Ultrasonics 42:943
109. Husseini GA, De la Rosa MA, Diaz T, Gabuji Y, Zeng DA, Christensen WG, Pitt J (2007) Nanosci Nanotechnol 7:1028
110. Kabanov AV, Batrakova EV, Miller DW (2003) Adv Drug Deliv Rev 55:151
111. Spitzenberger TJ, Heilman D, Diekmann C, Batrakova EV, Kabanov AV, Gendelman HE, Elmquist WF, Persidsky YJ (2007) Cereb Blood Flow Metab 27:1033
112. Batrakova E, Han H, Miller D, Kabanov A (1998) Pharm Res 15:1525
113. Batrakova E, Han H, Alakhov V, Miller D, Kabanov A (1998) Pharm Res 15:850
114. Kwon SH, Kim SY, Ha KW, Kang MJ, Huh JS, Im TJ, Kim YM, Park YM, Kang KH, Lee S, Chang JY (2007) Arch Pharm Res 30:1138
115. Alakhov V, Klinski E, Li S, Pietrzynski G, Venne A, Batrakova EV, Bronitch T, Kabanov A (1999) Colloids Surf B Biointerfaces 16:113
116. Kabanov A, Alakhov V (2002) Crit Rev Ther Drug Carrier Syst 19:1
117. Krupka TM, Weinberg BD, Wu H, Ziats NP, Exner AA (2007) Exp Biol Med (Maywood) 232:950
118. Kabanov AV, Chekhonin VP, Alakhov VY, Batrakova EV, Lebedev AS, Melik-Nubarov NS, Arzhakov SA, Levashov AV, Morozov GV, Severin ES, Kabanov VA (1989) FEBS Lett 258:343
119. Saski W, Shah SG (1965) J Pharm Sci 54:277
120. Saski W, Shah SG (1965) J Pharm Sci 54:71
121. Croy SR, Kwon G (2004) J Control Release 95:161
122. Croy SR, Kwon GS (2005) J Pharm Sci 94:2345
123. Lee ES, Oh YT, Seok Youn Yu YS, Nam M, Park B, Yun J, Kim JH, Ho-Taek S (2011) Colloids Surf A Biointerfaces 82:190
124. Kadam Y, Yerramilli U, Bahadur A, Bahadur P (2011) Colloids Surf B Biointerfaces 83:49
125. Sardar R, Funston AM, Mulvaney P, Murray RW (2009) Langmuir 25:13840
126. Giljohann DA, Seferos DS, Daniel WL, Massich MD, Patel PC, Angew CA (2010) Chem, Int Ed 49:3280
127. Homberger M, Simon U (2010) Philos Trans R Soc A 368:1405
128. Sperling RA, Gil PR, Zhang F, Zanella M, Parak W (1896) J Chem Soc Rev 2008:37
129. Jain PK, El-Sayed IH, El-Sayed MA (2007) Nanotoday 2:18
130. Bajpai SK, Mohan YM, Bajpai M, Tankhiwale R, Thomas VJ (2007) Nanosci Nanotechnol 7:2994
131. Goy-Lopez SE, Castro S, Taboada P, Mosquera V (2008) Langmuir 24:13186
132. Rahme K, Oberdisse J, Schweins R, Gaillard C, Marty JD, Mingotaud C, Gauffre F (2008) Chem Phys Chem 9:2230
133. Bakshi MS, Kaura A, Bhandari P, Kaur G, Torigoe K, Esumi KJ (2006) Nanosci Nanotechnol 6:1405
134. Sakai T, Alexandridis P (2006) Chem Mater 18:2577
135. Smart T, Lomas H, Massignani M, Flores-Merino MV, Perez LR, Battaglia G (2008) Nanotoday 13:38
136. Sakai T, Alexandridis P (2005) J Phys Chem B 109:7766
137. Durand-Gasselin C, Capelot M, Sanson N, Lequeux N (2010) Langmuir 26:12321
138. Ray D, Aswal VK, Srivastava DJ (2011) Nanosci Nanotechnol 11:1905
139. Ray D, Aswal VK, Srivastava DJ (2010) Nanosci Nanotechnol 10:6356
140. Ray D, Aswal VK, Kohlbrecher J (2011) Langmuir 27:4048
141. Khullar P, Mahal A, Singh V, Banipal TS, Kaur G, Bakshi MS (2010) Langmuir 26:11363
142. Su YL, Wei XF, Liu HZ, Colloid Interface J (2003) Sci 264:526
143. Bagshaw SA, Prouzet E, Pinnavaia TJ (1995) Science 269:1242
144. Zhao D, Huo Q, Feng J, Chmelka BF, Stucky GD (1998) J Am Chem Soc 120:6024
145. Kim HG, Oh C, Lee YH, Park SH, Oh SG (2007) J Ceramic Process Res 8:177
146. Huang Y, Cai H, Yu T, Sun X, Tu B, Zhao D (2007) Asian J 2:1282
147. da Silva MCH, da Silva LHM, Paggioli FJ (2005) Anal Sci 21:933
148. Li Y, Rojas OJ, Hinestroza JP (2012) Ind Eng Chem Res 51:2931
149. Hu J, Baglio V, Tricoli V, Aricò AS, Antonucci V (2008) J Appl Electrochem 38:543

doi:10.1186/2228-5547-4-12
Cite this article as: Singh *et al.*: **Micelles, mixed micelles, and applications of polyoxypropylene (PPO)-polyoxyethylene (PEO)-polyoxypropylene (PPO) triblock polymers.** *International Journal of Industrial Chemistry* 2013 **4**:12.